analytical chemistry

ARTICLE

pubs.acs.org/ac

Method for Optimizing Coating Properties Based on an Evolutionary Algorithm Approach

Davide Carta,[†,‡] Laura Villanova,[*,§,∥] Stefano Costacurta,[†] Alessandro Patelli,[†] Irene Poli,[‡,⊥] Simone Vezzù,[†] Paolo Scopece,[†] Fabio Lisi,[⊗] Kate Smith-Miles,[∥] Rob J. Hyndman,[○] Anita J. Hill,[⊗] and Paolo Falcaro[*,†,⊗]

[†]Associazione CIVEN, Via delle Industrie 5, 30175 Venezia, Italy

[‡]European Centre for Living Technology, Ca' Minich, San Marco 2940, 30124 Venezia, Italy

[§]Dipartimento di Scienze Statistiche, Università di Padova, Via Cesare Battisti 241, 35121 Padova, Italy

[∥]School of Mathematical Sciences, Faculty of Science, Monash University, Building 28, Wellington Road, Clayton, Australia

[⊥]Dipartimento di Statistica, Università Ca' Foscari di Venezia, San Giobbe, Cannaregio 873, 30121 Venice, Italy

[⊗]CSIRO, Materials Science & Engineering, Gate 5 Normanby Road, Clayton VIC 3168, Australia

[○]Department of Econometrics and Business Statistics, Faculty of Business and Economics, Monash University, Building 11, Wellington Road, Clayton, Australia

Supporting Information

ABSTRACT: In industry as well as many areas of scientific research, data collected often contain a number of responses of interest for a chosen set of exploratory variables. Optimization of such multivariable multiresponse systems is a challenge well suited to genetic algorithms as global optimization tools. One such example is the optimization of coating surfaces with the required absolute and relative sensitivity for detecting analytes using devices such as sensor arrays. High-throughput synthesis and screening methods can be used to accelerate materials discovery and optimization; however, an important practical consideration for successful optimization of materials for arrays and other applications is the ability to generate adequate information from a minimum number of experiments. Here we present a case study to evaluate the efficiency of a novel evolutionary model-based multiresponse approach (EMMA) that enables the optimization of a coating while minimizing the number of experiments. EMMA plans the experiments and simultaneously models the material properties. We illustrate this novel procedure for materials optimization by testing the algorithm on a sol−gel synthetic route for production and optimization of a well studied amino-methyl-silane coating. The response variables of the coating have been optimized based on application criteria for micro- and macro-array surfaces. Spotting performance has been monitored using a fluorescent dye molecule for demonstration purposes and measured using a laser scanner. Optimization is achieved by exploring less than 2% of the possible experiments, resulting in identification of the most influential compositional variables. Use of EMMA to optimize control factors of a product or process is illustrated, and the proposed approach is shown to be a promising tool for simultaneously optimizing and modeling multivariable multiresponse systems.

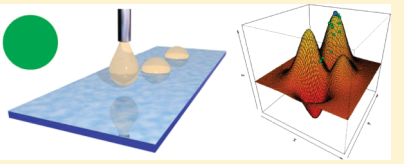

In many applications, the optimization of material properties is a fundamental process for the development and enhancement of new and existing technology. Material optimization is often a nontrivial process as materials scientists have to deal with multivariable multiresponse systems. In general, to optimize a system with multiple parameters it is necessary to perform experiments varying all of the variables simultaneously.[1] Despite this, the one-factor-at-a-time (OFAT) approach is the most commonly used in scientific and industrial practice. OFAT varies only one variable (factor) at a time keeping the others fixed.[2] Many scientists and engineers perform OFAT experiments because a trend in the response can be easily detected and related to changes in the compositional variables' values.[3] OFAT experiments are typically outperformed by techniques belonging to the field of the design of experiments (DOE).[1] However, standard DOE methods are often not suitable for the complexity that arises in material studies because chemical systems typically involve multiple responses, multiple interrelated variables, expensive experiments, and time-consuming material characterization procedures.[4]

In such a context, multiobjective evolutionary computing methods have emerged as successful for analytical technique optimization.[5] Promising results have also been achieved through the use of model-based methods[6−8] which approximate the unknown variable-response relations of the system, predict the response values at uninvestigated points and, eventually, suggest new experiments. Approximating models are typically assumed to be correct;[9] however, since real-world problems are often characterized by high dimensionality and lack of data, a sufficiently accurate model can be difficult to obtain. As a consequence, convergence to false optima may occur.[10] To overcome this drawback, Jin et al.[10] introduced the concept of evolution

Received: May 26, 2011
Accepted: July 5, 2011
Published: July 05, 2011

control which can include the measurement of the response values through practical experimentation, thus avoiding total reliance on the response values estimated by the approximating model.

In this work, we present a pioneering method, named evolutionary model-based multiresponse approach (EMMA). It employs a bioinspired evolutionary computation procedure (particle swarm optimization, PSO[11,12]), a statistical model (multivariate adaptive regression splines, MARS[13]), and an evolution control strategy. The PSO and the MARS model are used to suggest a set of new experiments. The collected data are then used to update the MARS model. The whole procedure is repeated until an optimal composition is approached, that is until EMMA consecutively suggests the same set of variable values. To avoid the identification of false optima, evolution control is introduced.[10] Because of the embedded modeling process, the method has the ability to identify the most influential variables of the system and to provide information about their relationships to the responses.

Use of this new method for optimization of a chemical system is illustrated through a case study in which a sol−gel recipe is optimized for use as a molecular grafting coating. The chosen chemical system is one that is well-studied and gives several feasible settings of the exploratory variables. The coating response features that are screened for optimization are chosen according to well documented application criteria for micro- and macro-array surfaces as detailed below. Application of the EMMA method in our case study is shown to provide the optimal setting of the variables to achieve the multiple response features simultaneously, thereby optimizing the surface chemistry for the chosen coating response features.

The chemical system chosen is an aminosilane recipe because although this chemical system has been extensively investigated,[14] the behavior of the solution and the coating properties are not precisely predictable. So for the purpose of this case study, this chemical system presents a valid test bed for the optimization method. In addition, the importance of amino functionalized surfaces in a wide range of applications makes this chemical system attractive for the case study, for example, such surfaces are important in electrical, electrochemical, and optical sensors,[15−18] robotic microhandling,[19] biocompatibilization,[20] immunoassay,[21] biochips,[22] biocatalytic systems,[23] high density devices,[24] facilitating agents for metal organic framework nucleation,[25] and perm-selective devices.[26,27] In our case study, sol stability is one of the responses chosen as critical for coating optimization. Rapid gelation has been shown to have a dramatic effect on coating properties (homogeneity, grafting capacity, thickness) due to the influence of the aminosilane on the cross-linking rate of the siloxane units.[28,29] Sol−gel methods that result in reproducible amino-functionalized films have been reported by several groups.[30−32] In our study, we use the approach presented by Oh and co-workers[32] who prepared dense reproducible amino-functionalized coatings by adding butyltrimethoxysilane as a coreactant. Oh et al.[32] investigated their surfaces for use in DNA microarrays. Their study indicated that the surface amine density is not the sole determining factor for the efficiency of the array in discriminating the perfectly matched target oligodeoxynucleotide from the single mismatched ones. Their results suggest that coating optimization might be possible based on controlling spacer linker lengths in order to separate the amino-groups. Their conclusions prompt an investigation of the controlling factors for coating efficiency in the microarray application, making this chemical system and application well-suited for our case study.

A micro- or macro-array is a small analytical device designed for fast and precise detection of analytes through binding events that immobilize interacting elements on a few square micrometers. Microarrays have spot sizes <250 μm; macroarrays have spot sizes >300 μm.[33] Such technology employs a glass slide substrate with targets (biomolecules such as cDNA, oligonucleotides, RNA, proteins, antibodies) grafted in specific positions (array). A solution with fluorescent dye-labeled biomolecules (reporter molecules or probes) is spotted onto the slide. If the probe represents the complementary interacting element, then binding and immobilization occurs.[34] The glass slide is then rinsed to remove the unreacted compounds. A laser scanner measures intensity and position of the fluorescent signal corresponding to the bonded dye-labeled molecules (spot) and the collected data contain information about interaction partners. Microarrays are a very promising analytical tool for diagnostic assays;[34] however, concerns about reproducibility and low sensitivity of this technique still remain.[35−38] Wang et al.[39] highlighted that the main source of inherent variability in the expression data is strongly affected by the spot quality. Schena stated that "a microarray experiment is only as good as the surface that is used to create it".[34] Hence it is well recognized that coating engineering can play a significant role in the fabrication of sensitive and reliable microarrays. Angenendt[37] and Kusnezow et al.[38] compared the performance of several different surface coatings for protein and antibody microarrays on coated glass slides using the OFAT approach, standard microarray instrumentation, fluorescent reporter molecules in the spotting solution, and using the measured spot signal intensity, background level, and spot morphology (evaluated visually) as measures of coating performance. The criteria for coating performance responses that will be screened in our case study to drive coating optimization have been developed based on automatic or semiautomatic microarray image processing methods. Ideal spots are perfectly circular and identical, characterized by uniform background, homogeneous density of probe molecules, and high signal-to-noise ratio.[39−42] The background fluorescence generated by a nonoptimized coating (low signal-to-noise ratio) might induce a systematic error even if laser scanner images are analyzed with commercial software.[43] Most of the automatic and semiautomatic methods for spot recognition assume both a perfect circularity of the spot and a difference between the spot and the background intensity;[44] however, these assumptions are not always valid, and irregularity of the spot shape can largely compromise the accuracy of the measurements.[44]

On the basis of this background knowledge of the important variables and response factors, our case study will optimize an amino-methyl-silane coating by varying six compositional variables to optimize five responses. The compositional variables are tetraethoxysilane (TEOS), aminopropyltriethoxysilane (APTES), methyltriethoxysilane (MTES), ethanol (EtOH), HCl, and H_2O; the responses are the pot life (stability of the solution, S_t) and the quality of the sol−gel coating (as defined by spot shape S, spot intensity I_M, background intensity I_B, and spot homogeneity H).

Spotting performance has been monitored using a fluorescent dye molecule (fluorescein isothiocyanate, FITC) as the reporter molecule in our case study. Because the dye selectively grafts the amino-functionality of the coating, luminescent spots are obtained that can be rapidly screened using a microarray laser scanner. This choice of dye has been motivated by the desire to use an established grafting procedure[45] to test the EMMA algorithm. This choice allows us to benchmark our EMMA case

study results against coating performance reported previously that was optimized by OFAT changing one variable at a time.[45] The algorithm would possibly require being adapted if a biological assay were used; in fact, in that case, other important features would need to be screened for optimization (e.g., nonspecific binding, intra- and inter-assay reproducibility, etc.).[46]

EXPERIMENTAL SECTION

Materials and Measurements. The detailed procedure for coating preparation is reported in the Supporting Information (S1). After addition of EtOH, TEOS, MTES, H_2O, and HCl, the solution is stirred for 15 min. APTES is then added, and the solution is stirred for a further 20 min (aging time). Information on the stability of the sol is collected with a variable (stability, S_t), which is 0 if gelation occurs within 20 min aging or 1 if the sol remains transparent (no gelation within the aging time). The surface grafting is tested using FITC (Figure 1a). The coating is spotted with a FITC doped standard microarray buffer solution (FITC-buffer solution). Controlled pumping rate of the spotting solution allows for the formation of circular spots mimicking the method used in micro- and macro-array technology (Figure 1b). Three images related to three independent tests are collected by analyzing each slide with a microarray scanner. The green color of the spot is due to the intense fluorescent signal of the FITC molecules bound to the amino groups of the coating surface. Some streaking is evident due to the FITC molecules bonding with amino groups during the rinsing process.

Figure 1c−h shows the analysis procedure for spots illustrating the procedure for two different coatings. The response functions S, I_M, I_B, and H are measured as described here. A circle with the largest possible area (yellow dotted circle) is inscribed in each spot allowing for the definition of a center (C) and a minimum radius (min_R) (Figure 1e,f). A point along the perimeter of the spot shape (P) is then chosen in order to define the maximum distance CP (max_R). The min_R/max_R ratio (S) measures the spot circularity, and in the case of a perfect circle, then $S = 1$. The background intensity parameter (I_B) is selected by averaging 60 intensity measurements along the blue-dashed circumference ($^4/_3$ of the maximum dimension of the spot; see Figure 1e,f). The spot intensity (I_M) is calculated averaging the fluorescence intensity values inside the yellow-dotted circular area. Three different intensities with the maximum values (yellow pointers in Figure 1g,h) are averaged giving the value H_M. Three different pixels with the minimum values (red pointers) are averaged calculating H_m. The minimum to maximum intensity ratio (H_m/H_M) defines the homogeneity of the intensity signal inside the spot (H).

Methods. The compositional range has been selected in accordance with preliminary experiments to evaluate the pot lifetime of the sol−gel solution, resulting in the selection of a set of six possible amounts of moles for TEOS, APTES, MTES, EtOH, HCl, and H_2O (values reported in the Supporting Information, Table S2_T1). EMMA defines an experiment by selecting the amounts of moles for each compositional variable. The algorithm evolves with cycles depending on a parameter t, named the time instant. When $t = 0$, EMMA selects 48 random recipes for the sol−gel recipe ("experiments"). When $t > 0$, EMMA evolves the initial experiments by changing the number of moles of the chemical components. Once a set of sol−gel recipes are defined, the solutions are prepared and the coatings deposited. The coated slides are then spotted using the FITC-buffer solution and I_M, S, I_B, and H are measured. Then, EMMA identifies the best experiments and selects a new set of recipes

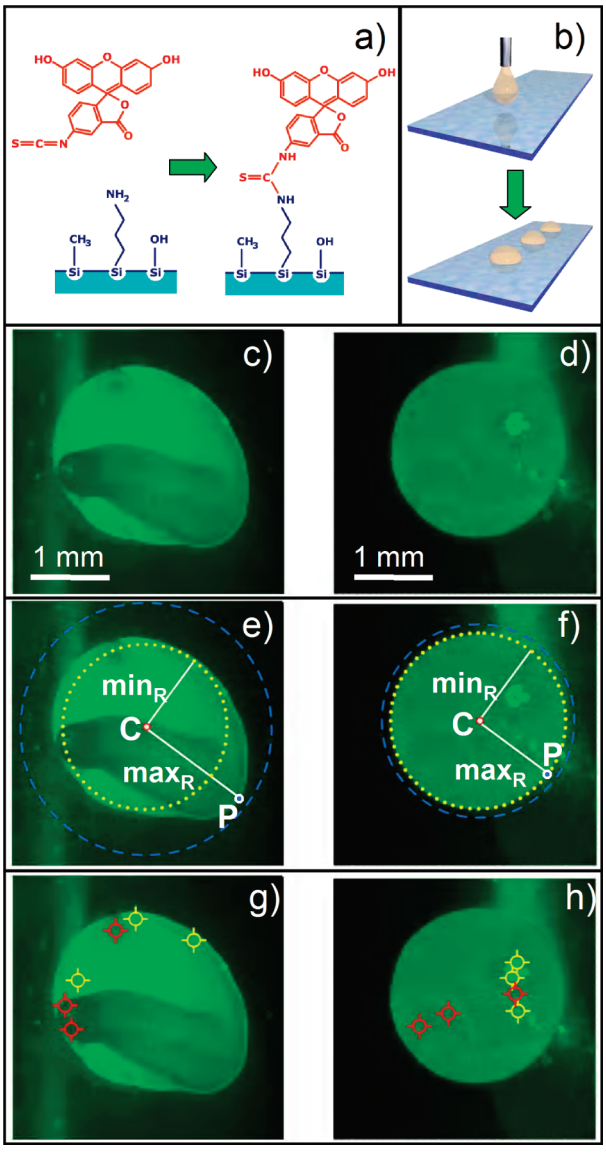

Figure 1. (a) Reaction between the isothiocyanate group of the demonstration dye fluorescein isothiocyanate FITC (red) with the amino functionality of the amino-methyl-silane coating and (b) schematic representation of the spotting process. The needle−substrate distance and pumping rate are kept constant; and the volume of the drop is fixed. (c,d) Examples of two different spots generated by two different amino-methyl-silane coatings. (e,f) Graphical procedure to determine the circularity (S). A circle with the largest possible area is inscribed in each spot allowing for the definition of a center (C) and a minimum radius (minR). A point along the perimeter of the spot shape (P) is then chosen in order to define the maximum distance CP (maxR). The minR/maxR ratio (S) measures the spot circularity. If minR/maxR = 1, the spot is perfectly circular (f). The background intensity parameter (I_B) is measured by averaging 60 intensity measurements along the blue dashed circumference (about $^4/_3$ of the maximum dimension of the spot). The spot intensity (I_M) is calculated by averaging the fluorescence intensity values inside the yellow dotted circular area. (g,h) Three different intensities with the maximum values (yellow pointers) are averaged giving the value H_M. Three different pixels with the minimum values (red pointers) are averaged calculating H_m. The minimum to maximum intensity ratio (H_m/H_M) within the circumference defines the homogeneity of the intensity signal inside the spot (H).

dx.doi.org/10.1021/ac201337e |*Anal. Chem.* 2011, 83, 6373–6380

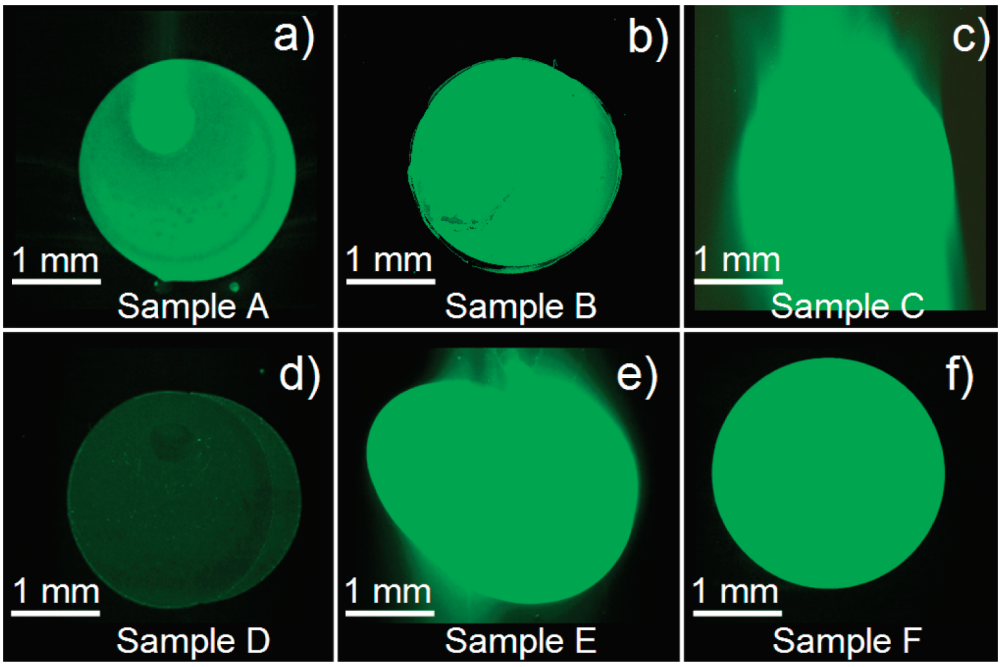

Figure 2. Laser scanner measurements of spots on different amino-methyl-silane coatings. The sample with the best features found using the OFAT approach is sample A (a). From Sample B to F, different spots found during the evolution of the algorithm are presented. The sample with the best features found by EMMA is sample F (f) presenting an improved signal-to-noise ratio, homogeneity, and perfect circular shape. For all of the samples shown here, the full response sets are reported in the Supporting Information (Table S5_T1).

(see flowchart S2_F1 in the Supporting Information). In EMMA, a weight has been assigned to each response; the weights are user-defined values and correspond to 0.4 for I_M and S, 0.12 for I_B, and 0.08 for H. A total of 123 sol−gel recipes were investigated: 48 for $t = 0$ and 15 for $t = 1,...,5$ (a simulation and examples of the obtained coatings can be found in Algorithm and Coating Features). When $t > 0$, the number of recipes prepared for each time instant was reduced to 15 in order to test the algorithm efficiency at optimizing the coating while performing less than 2% of all the possible experiments. Empirical preliminary studies have supported this decision (see the Supporting Information, S3).

The collected data have been analyzed by EMMA. The method determines the influence of each variable on each coating response and models the functional relationships between compositional variables and coating features using a classification tree to investigate the response S_t (see the Supporting Information, S4). The performance of the each new coating selected by EMMA has been compared with the best coating obtained with the OFAT approach, identified in previous work.[45] In that work, the first criterion was a sol−gel solution with a pot life longer than 20 min. Once this criterion was achieved, approximately 70 solutions were prepared in order to improve the coating properties by changing one variable at a time and the experiments were stopped when no further progress was detected for any change of each variable. This OFAT approach will be used to benchmark EMMA in our case study.

RESULTS

After identification of the best coating obtained by EMMA, a small number of additional experiments have been performed, systematically changing the quantity of one reactant while keeping the others fixed. Because no further improvement in performance was measured, the performance of the best coating obtained using EMMA was compared with the best coating obtained using the OFAT approach. The spot features (S_t, S, I_M, I_B, H) measured on the prepared coatings have been used as input in the algorithm for modeling. The models describing the system behavior are discussed in Modeling the Results.

Algorithm and Coating Features. The theoretical efficiency of the proposed approach has been verified using a simulation based on a preliminary experimental model (48 recipes evaluated, see the Supporting Information, S3). Then, 15 new experiments were selected for each subsequent time instant. Each time instant involves experiment identification, solution preparation, coating deposition, and spot analysis.

Figure 2a presents the laser scanner measurement of a spot obtained by the best coating (sample A) found with the OFAT methodology. Tests performed using drops of FITC-buffer solution on this coating give perfectly circular spots ($S = 1$). However, the fluorescence signal is weak with a partial inhomogeneous distribution.

Examples of coatings obtained using EMMA are shown in Figures 2b−f (samples B−F). The calculated spot features shown in Figure 2 are reported in the Supporting Information (Table S5_T1). Coating B (Figure 2b) has the same circularity, better homogeneity and a stronger intensity for I_M and I_B, compared to coating A. Sample C (Figure 2c) gives I_M and I_B ~3 times more intense than sample A, and the ratio $I_M/I_B \sim 4.5$ is similar; although the spot (Figure 2c) is almost circular, poor homogeneity is measured. Sample D (Figure 2d) shows very low background and good homogeneity but has a spot intensity similar to the background and an irregular shape. Sample E (Figure 2e) shows a homogeneous fluorescence signal with intensity values similar to those found for sample A but has poor

circularity and high background. Sample F (Figure 2f) represents the best result found by EMMA: perfect circular shape, signal with intense and homogeneous features, and low background fluorescence. The intensity I_M of the spot measured in sample F is 380% more intense than that detected for sample A. Because intensity can be assumed to be proportional to the number of fluorophores (employing the same measurement parameters),[47] sample F shows a significantly improved capacity for grafting dye molecules over our benchmark sample A. The 139% increase in background intensity (I_B) can be explained by two different reasons: (1) a higher weight has been given in EMMA to improve I_M compared to I_B (respectively, 0.4 and 0.12), (2) the improved ability to graft dye molecules that increases I_M is reflected also in I_B in that during the rinsing process the unreacted dye in the spot is solubilized by the solvent, and grafting can occur on the coating surface during the rinse. Therefore, a combined effect relating I_B to I_M is expected. However, the improvement in terms of signal-to-noise ratio (I_M/I_B) is 273%. No changes were detected in the perfect circular shape ($S = 1$). An explanation is that the circularity weight is 0.4; therefore, EMMA keeps the circular shape as one of the most important features. A 188% improvement has been obtained for homogeneity (H).

Ellipsometry and contact angle measurements for the coatings are reported in the Supporting Information, S5. Weak correlations between the coating thickness and I_M , and between the contact angle and I_B were found. The remaining combinations of S, I_M, I_B, and H versus contact angle, refractive index, and coating thickness do not exhibit any simple trend. Also, no simple correlation between chemical species and coating properties has been found using FT-IR spectroscopy. For this reason we have modeled the coating features as functions of the compositional variables using a statistical approach.

Modeling the Results. We used a classification tree model to investigate the stability variable (Supporting Information, S4_F1). For an experimentalist, it can be very difficult to define the range of multivariables that will give sol stability using the OFAT approach. The model defines MTES, APTES, and H_2O as the most relevant compositional variables affecting the solution stability and predicts with 92% probability a stable composition (pot life >20 min) under one of the following conditions: (i) MTES $\geq 0.7 \times 10^{-3}$ M; (ii) MTES $< 7 \times 10^{-3}$ M and APTES $< 0.8 \times 10^{-3}$ M; (iii) MTES $< 7 \times 10^{-3}$ M, APTES $\geq 0.8 \times 10^{-3}$ M, and $H_2O < 51.5 \times 10^{-3}$ M. These classification tree model results can be better understood based on literature results that show that MTES reduces the network connectivity due to the nonhydrolyzable Si-CH_3 groups,[48,49] and it therefore plays a central role in sol stabilization.

EMMA determined the influence of each variable on the different responses by modeling the relations between compositional variables and responses. The use of the MARS model and the procedure to calculate the influence of compositional variables are presented in the Supporting Information, S6 and S7. APTES and EtOH strongly affect I_M, whereas HCl is less influential. APTES also heavily influences I_B: a higher concentration of amino groups increases the coating's ability to bind solubilized dye molecules during the rinsing process as illustrated by luminescence streaks (see Figure 1c,d). S (circularity) is largely influenced by the amount of MTES, with a larger amount of MTES associated with more circular spots. H (homogeneity) is mainly affected by HCl.

A MARS model has been obtained for each response. The MARS model identifies independent and combined interactions as shown in Figure 3, where the influence of the most important compositional variables on I_M, I_B, H, and S are presented. Each graph presents a modeled coating feature at a given time instant, whereas the optimized coating (sample F) is the result of a combination of four features maximized simultaneously. Sample F has been obtained in accordance with the imposed weight for each response, as previously described.

In Figure 3a−d, I_M is described in terms of APTES, EtOH, HCl, and their combined interactions with other variables. Figure 3a shows that by increasing the amount of APTES, the intensity I_M increases. A maximum occurs at the value ln-(APTES) = −7.14 (corresponding to 0.79×10^{-3} M), and then a further increase of the aminosilane produces a decrease of I_M. This graph shows that APTES can itself strongly affect the spot intensity. In the 0.21 to 0.79 mM range, I_M increases from 0.5 to 1.99, meaning that a 400% improvement in the intensity can be achieved just by optimizing the APTES amount. The concentration of reporter molecules (FITC) has been kept constant in our case study. Schena has reported that for a fixed surface chemistry a maximum in spot intensity is observed when the reporter molecule concentration is optimized.[34] These results highlight the potential of future applications of EMMA to develop microarray surfaces for optimal binding where both the concentration of reporter molecules and surface binding sites are allowed to vary simultaneously. In Figure 3b, the interaction between APTES and EtOH is shown. Two maxima can be found at A (−1.88,−7.14) and B (−0.69,−6.17), corresponding to (0.15, 0.79×10^{-3}) M and (0.501, 2.09×10^{-3}) M. At ln(APTES) = −7.14, decreasing the amount of EtOH, I_M increases to 4.43 (absolute maximum, point A in Figure 3b). A relative maximum (I_M = 1.69, point B in Figure 3b) can be found by keeping the solvent concentration constant, ln(EtOH) = −0.69 and increasing the concentration of amino groups. Figure 3c shows the ethanol−water interaction: amounts of H_2O below 0.0146 M ($\ln(H_2O)$ = −4.23) and amounts of EtOH below 0.501 M (ln(EtOH) = −0.69) result in a dramatic decrease of I_M. For $\ln(H_2O)$ in the −4.23 to −1.97 range, I_M can be varied in the 0.86 to 2.83 range by just changing the amount of EtOH. Figure 3d shows the combined effect of HCl and H_2O. A plateau with intensity around 1.55 is found for HCl amounts below 0.43×10^{-3} M (ln(HCl) = −7.76) and H_2O amounts above 0.025 M ($\ln(H_2O)$ = −3.67). Outside this compositional range, the intensity decreases quickly.

APTES and EtOH were found to be the most important variables in modeling I_M. This result can be better understood in the context of its agreement with literature reports of the selective binding between FITC and APTES molecules.[45] Regarding EtOH, a study performed by Harris et al.[50] confirms a similar trend, revealing the importance of ethanol on dye adsorption in pure silica sol−gel coatings. In that study, the coating with the lowest EtOH/TEOS ratio shows the greatest adsorption of dye. The amount of solvent determines the dilution of the precursor solution, which has important effects such as slowing down the kinetics of hydrolysis and polycondensation at higher amounts of ethanol;[50] lower EtOH concentrations result in thicker coatings.[50] These results are consistent with the observed direct proportionality between maximum spot intensity and coating thickness observed in our case study (Supporting Information, S5_F1).

The model for I_B prioritizes the APTES contribution and its combined effect with other variables (HCl and MTES). In Figure 3e, a maximum with I_B = 2.09 corresponds to ln(APTES) = −6.89 (1.02×10^{-3} M), then a further increase of aminosilane decreases the background signal. APTES interacts with HCl as shown in Figure 3f. In Figure 3g the combined effect of MTES and APTES is

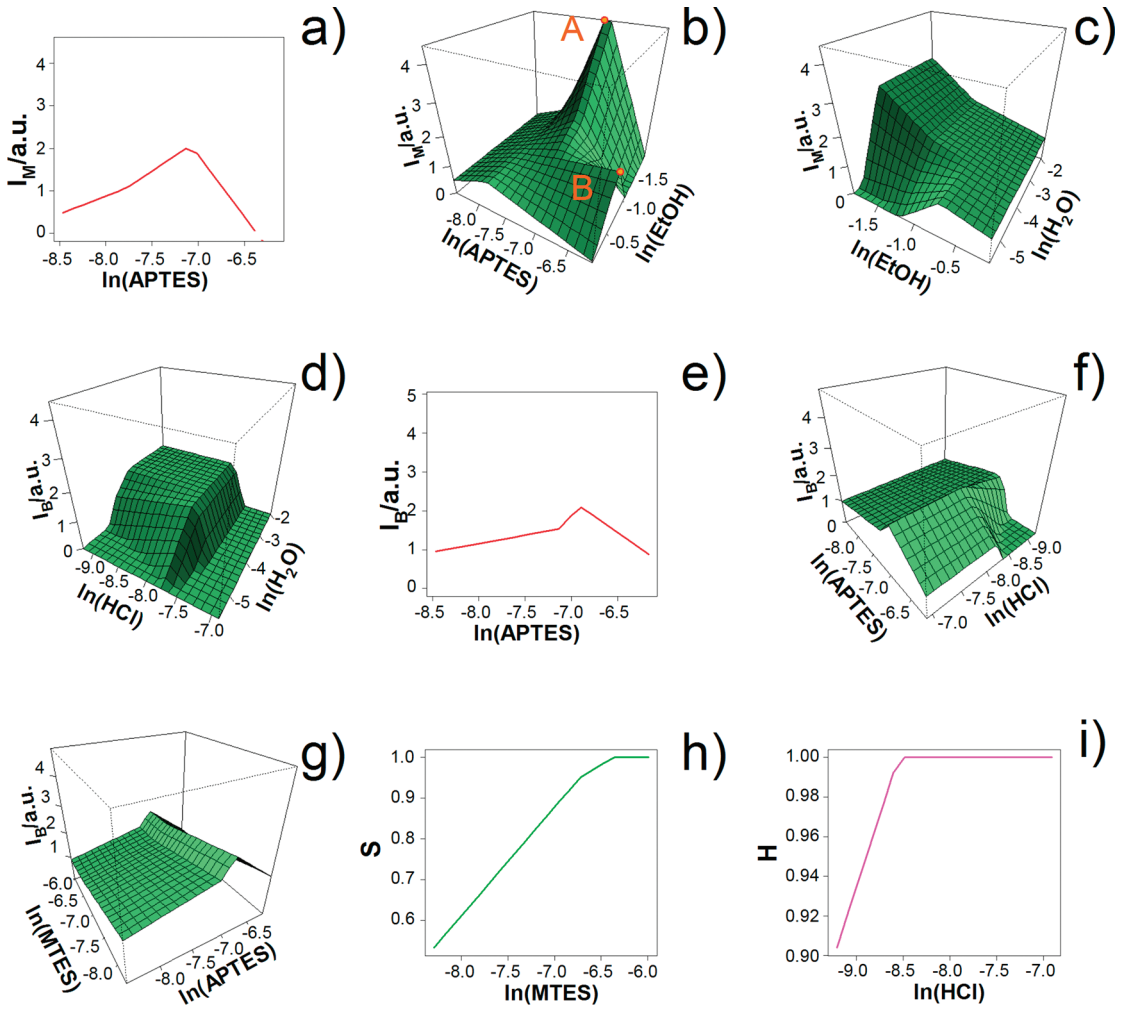

Figure 3. Model provided by EMMA explaining the relationships between compositional variables and optimized responses. Multicollinearity issues can be excluded (see the Supporting Information, S8). I_M was related with a single interaction to APTES (a), and with a combined interaction to APTES and EtOH (b), EtOH and H_2O (c), and HCl and H_2O (d). I_B was related with a single interaction to APTES (e), and with combined interactions to APTES and HCl (f), and MTES and APTES (g). *S* was related with a single interaction to MTES (h). *H* was related with a single interaction to HCl (i).

presented: this profile is in agreement with the trend depicted in Figure 3e and the background signal decreases if the amount of MTES is increased.

The I_B trend (Figure 3e) is similar to the APTES contribution shown for I_M (Figure 3a); this result supports the hypothesis relating I_M to I_B and explains the higher background signal in the best coating found with the EMMA approach. However, the two maxima occur at slightly different values of ln(APTES), such that I_M/I_B can be optimized. The signal-to-noise ratio can also be improved by varying the amount of solvent (as discussed previously for I_M) or by increasing the amount of methyl groups (as shown for I_B). An increasing density of methyl groups increases the hydrophobic properties of the substrate, as illustrated by the plot of I_B versus contact angle (Supporting Information, S5_F2).

MTES is the most influential variable for spot circularity (*S*). Figure 3h shows that increasing the amount of MTES allows reaching the best theoretical value ($S = 1$), which is obtained for quantities of ln(MTES) greater than -6.36 (1.7×10^{-3} M). The crucial effect of MTES can be attributed to the hydrophobicity induced by methyl groups, which results in a lower affinity between the surface and the FITC-buffer solution drop. During the binding process, the dye solution evaporates leaving a circular mark, whereas for coatings with high wettability the drop spreads on the surface, leaving a poorly defined shape.

As shown in Figure 3i, spot homogeneity, *H*, improves slightly for ln(HCl) > -9.21 (0.1×10^{-3} M), reaching $H = 1$ for ln(HCl) > -8.48 (0.2×10^{-3} M), then stabilizes for a wide range of HCl concentration.

To verify the optimized recipe and the relationships predicted between compositional variables, a set of 25 experiments have been performed in the space surrounding the identified optimum. The prepared coatings present responses in agreement with the algorithm prediction. The measured experimental coating responses are within 10% of the values calculated using the model. The optimum coating has been reproduced 5 times (once a week for 5 weeks). The variations in response around the mean are all within 2 standard deviations, with the exception of one measurement of I_M in one sample only which slightly exceeds 2σ.

CONCLUSIONS

A new evolutionary bioinspired algorithm EMMA to solve multivariable multiresponse optimization problems has been

dx.doi.org/10.1021/ac201337e |*Anal. Chem.* 2011, 83, 6373–6380

illustrated using a case study. A sol−gel amino-methyl-silane coating has been optimized for immobilization of a fluorescent dye molecule. In the case study, EMMA was shown capable of varying six compositional variables (reactants) simultaneously to design experiments and optimize five responses (coating features) of the system while minimizing the number of experiments. PSO[11,12] and MARS[13] were used to suggest a set of sol−gel recipes and maintain balance between exploration (global search) and exploitation (local search) of the experimental space. In the experimental domain of the case study, the evolution control strategy constituted synthesis of the suggested sol−gel recipes and measurement of the resultant coating performance. The collected data (sol−gel compositions and coating quality measurements) were then used to update the MARS model. The whole procedure was repeated until an optimal composition was achieved. Remarkably, this new analytical method was able to optimize the system with less than 2% of the entire combination of possible experiments, resulting in the identification of the most influential compositional variables and describing both single and combined interactions between chemical reactants and coating responses.

EMMA was benchmarked against experimental optimization based on the OFAT approach. EMMA provided a significantly improved coating recipe resulting in high-quality spots for rapid screening using a microarray laser scanner: the signal-to-noise ratio was improved by 270%, the homogeneity was enhanced by 190%, and the shape was maintained as perfectly circular. Furthermore, EMMA defined aminosilane, methylsilane, ethanol, and hydrochloric acid as prominent variables to control the coating properties. These model results were discussed in the context of *a priori* knowledge and literature results for sol−gel coating property relationships. A classification tree has been employed to define the rules to efficiently predict stable solutions (percentage of correct classification equal to 92%). This study has successfully demonstrated EMMA as a new analytical tool for the optimization of material science problems that simultaneously provides fundamental information leading to a better understanding of the investigated system.

■ ASSOCIATED CONTENT

Supporting Information. Additional information as noted in text. This material is available free of charge via the Internet at http://pubs.acs.org.

■ AUTHOR INFORMATION

Corresponding Author

*E-mail: paolo.falcaro@csiro.au (P.F.); laura.villanova@stat.unipd.it (L.V.).

■ ACKNOWLEDGMENT

D.C. and L.V. contributed equally to this work.

■ REFERENCES

(1) Montgomery, D. C. *Design and Analysis of Experiments*; Wiley: Hoboken, NJ, 2009.
(2) Czitrom, V. *Am. Stat.* **1999**, *53*, 126.
(3) Daniel, C. *J. Am. Stat. Assoc.* **1973**, *68*, 353.
(4) Lau, D.; Hay, D. G.; Hill, M. R.; Muir, B. W.; Furman, S. A.; Kennedy, D. F. *Comb. Chem. High Throughput Screening* **2011**, *14*, 28.
(5) O'Hagan, S.; Dunn, W. B.; Brown, M.; Knowles, J. D.; Kell, D. B. *Anal. Chem.* **2005**, *77*, 290.
(6) O'Hagan, S.; Dunn, W. B.; Knowles, J. D.; Broadhurst, D.; Williams, R.; Ashworth, J. J.; Cameron, M.; Kell, D. B. *Anal. Chem.* **2007**, *79*, 464.
(7) Emmerich, M; Beume, N.; Naujoks, B. *Lecture Notes Comput. Sci.* **2005**, *3410*, 62.
(8) Knowles, J. *IEEE Trans. Evolut. Comput.* **2005**, *10*, 50.
(9) Jones, D. R. *J. Global Optim.* **2001**, *21*, 345.
(10) Jin, Y.; Olhofer, M.; Sendhoff, B. *IEEE Trans. Evolut. Comput.* **2002**, *6*, 481.
(11) Kennedy, J.; Eberhart, R. *IEEE International Conference on Neural Networks*, 1995; 1942.
(12) Villanova L.; Falcaro P.; Carta D.; Poli I.; Hyndman R.; Smith-Miles K. *IEEE Congress on Evolutionary Computation*, 18−23 July 2010, 1−8, DOI: 10.1109/CEC.2010.5586165.
(13) Breiman, L; Friedman, J. H. *J. R. Stat. Soc., Ser. B: Stat. Methodol.* **1997**, *59*, 3.
(14) Metwalli, E.; Haines, D.; Becker, O.; Conzone, S.; Pantano, C. G. *J. Colloid Interface Sci.* **2006**, *298*, 825.
(15) Shin, J. H.; Weinman, S. W.; Schoenfisch, M. H. *Anal. Chem.* **2005**, *77*, 3494.
(16) Lev, O.; Wu, Z.; Bharathi, S.; Glezer, V.; Modestov, A.; Gun, J.; Rabinovich, L.; Sampath, S. *Chem. Mater.* **1997**, *9*, 2354.
(17) Tonlé, I. K.; Diaco, T.; Ngameni, E.; Detellier, C. *Chem. Mater.* **2007**, *19*, 6629.
(18) Bakker, E. *Anal. Chem.* **2004**, *76*, 3285.
(19) Dejeu, J.; Gauthier, M.; Rougeot, P.; Boireau, W. *ACS Appl. Mater. Interfaces* **2009**, *1*, 1966.
(20) Colilla, M.; Salinas, A. J.; Vallet-Regí, M. *Chem. Mater.* **2006**, *18*, 5676.
(21) Sivagnanam, V.; Song, B.; Vandevyver, C.; Gijs, M. *Anal. Chem.* **2009**, *81*, 6509.
(22) Jang, L.-S.; Liu, H.-L. *Biomed. Microdevices* **2009**, *11*, 331.
(23) DeLouise, L. A.; Miller, B. L. *Anal. Chem.* **2004**, *76*, 6915.
(24) Martínez, R. V.; Martínez, J.; Chiesa, M.; Garcia, R.; Coronado, E.; Pinilla-Cienfuegos, E.; Tatay, S. *Adv. Mater.* **2010**, *22*, 588.
(25) Buso, D.; Nairn, K. N.; Gimona, M.; Hill, A. J.; Falcaro, P. *Chem. Mater.* **2011**, *23*, 929.
(26) Fattakhova-Rohlfing, D.; Wark, M.; Rathousky, J. *Chem. Mater.* **2007**, *19*, 1640.
(27) Calvo, A.; Angelomé, P. C.; Sanchez, V. M.; Scherlis, D. A.; Williams, F. J.; Soler-Illia, G. J. A. A. *Chem. Mater.* **2008**, *20*, 4661.
(28) Riegel, B.; Blittersdorf, S.; Kiefer, W.; Hofacker, S.; Muller, M.; Schottner, G. *J. Non-Cryst. Solids* **1998**, *226*, 76.
(29) Riegel, B.; Kiefer, W.; Hofacker, S.; Schottner, G. *J. Sol-Gel Sci. Technol.* **1998**, *13*, 385.
(30) Soler-Illia, G. J. A. A.; Angelomé, P. C.; Bozzano, P. B. *Chem. Commun.* **2004**, 2854.
(31) Calvo, A.; Fuertes, C. M.; Yameen, B.; Williams, F. J.; Azzaroni, O.; Soler-Illia, G. J. A. A. *Langmuir* **2010**, *26*, 5559.
(32) Oh, J. S.; Cho, S. J.; Kim, C. O.; Park, W. J. *Langmuir* **2002**, *18*, 1764.
(33) Angenendt, P. *Drug Discovery Today* **2005**, *10* (7), 503.
(34) Schena, M. *Microarray Analysis*; John Wiley & Sons: Hoboken, NJ, 2003.
(35) Couzin, J. *Science* **2006**, *313*, 1559.
(36) Marshal, E. *Science* **2004**, *306*, 630.
(37) Angenendt, P.; Glökler, J.; Murphy, D.; Lehrach, H.; Cahill, D. J. *Anal. Biochem.* **2002**, *309*, 253.
(38) Kusnezow, W.; Jacob, A.; Walijew, A.; Diehl, F.; Hoheisel, J. D. *Proteomics* **2003**, *3*−*3*, 254.
(39) Wang, X.; Ghosh, S.; Guo, S. W. *Nucleic Acids Res.* **2001**, *29*, e75.
(40) Giannakeas, N.; Fotiadis, D. I. *Comput. Med. Imaging Graph.* **2009**, *33*, 40.
(41) Dufva, M. *Biomol. Eng.* **2005**, *22*, 173.
(42) Hessner, M. J.; Meyer, L.; Tackes, J.; Muheisen, S.; Wang, X. *BMC Genomics* **2004**, *5*, 1.

(43) Sasik, R; Woelk, C. H.; Corbeil, J. *J. Mol. Endocrinol.* **2004**, *33*, 1.
(44) Kambhampati, D. *Protein Microarray Technology*; Wiley-VCH: Weinheim, Germany, 2003.
(45) Falcaro, P.; Malfatti, L.; Vaccari, L.; Amenitsch, H.; Marmiroli, B.; Grenci, G.; Innocenzi, P. *Adv. Mater.* **2009**, *21*, 4932.
(46) Wolter, A.; Niessner, R.; Seidel, M. *Anal. Chem.* **2008**, *80*, 5854.
(47) Lyng, H.; Badiee, A.; Svendsrud, D. H.; Hoving, E.; Myklebost, O.; Stokke, T. *BMC Genomics* **2004**, *5*, 10.
(48) van Bommel, M. J.; Bernards, T. N.; Boonstra, A. H. *J. Non-Cryst. Solids* **1991**, *128*, 231.
(49) Innocenzi, P; Abdirashid, M. O.; Guglielmi, M. *J. Sol-Gel Sci. Technol.* **1994**, *4*, 47.
(50) Harris, T. M.; Knobbe, E. T. *J. Mater. Sci. Lett.* **1996**, *15*, 153.